



4th International Conference on Silicon Photovoltaics, SiliconPV 2014

## A roadmap for PERC cell efficiency towards 22%, focused on technology-related constraints

Pietro P. Altermatt<sup>a</sup>, Keith R. McIntosh<sup>b</sup>

<sup>a</sup> Dep. Solar Energy, Inst. Solid-State Physics, Leibniz University Hannover, Appelstr. 2, 30167 Hannover, Germany

<sup>b</sup> PV Lighthouse, Coledale, 2512 NSW, Australia

---

### Abstract

Presently, the crystalline silicon (c-Si) photovoltaic (PV) industry is switching from standard cells to PERC cells to increase cell efficiency from about 18% to about 20%. This paper gives a roadmap for increasing PERC cell efficiency further towards 22%. Which equipment and which process conditions are feasible to go beyond 20% efficiency? To help answer this as generally as possible, we conduct state-of-the-art modelling in which we sweep the inputs that represent major *technology-related constraints*, such as diffusion depth, metal finger width and height, alignment tolerances, etc. (these are assigned to the x- and y-axes of our graphs). We then predict the *optimum device parameters resulting from these restrictions* (shown as contour lines). There are many different ways to achieve 22%. Our modelling predicts, for example, that 60  $\mu\text{m}$  wide screen-printed metal fingers are sufficiently narrow if the alignment tolerance (width of the  $n^{++}$  region) is below 90  $\mu\text{m}$ . The rear may be contacted with 30  $\mu\text{m}$  wide openings of the  $\text{Al}_2\text{O}_3/\text{SiN}_x$  stack and with local  $J_{0,\text{BSF}}$  values as high as 900  $\text{fA}/\text{cm}^2$ . If these requirements cannot be met, they may be compensated by improvements in other device parts. Regardless of this, the wafer material requires a SRH lifetime of at least 1 ms at excess carrier densities near  $10^{14} \text{cm}^{-3}$ .

© 2014 Published by Elsevier Ltd. This is an open access article under the CC BY-NC-ND license

(<http://creativecommons.org/licenses/by-nc-nd/3.0/>).

Peer-review under responsibility of the scientific committee of the SiliconPV 2014 conference

*Keywords:* Device modeling; PERC cells; roadmap

---

### 1. Evolutionary or revolutionary development?

In the past, the c-Si PV industry went from 14% to 18% efficiency on an evolutionary path, where only single fabrication processes were optimised or altered. It is presently going from about 18% towards 20% by switching from standard cells to PERC cells. The switch cannot be achieved by an evolutionary approach, because both the front and the rear must be improved at the same time to make PERC design effective. Therefore, PERC cells need some new fabrication equipment. We show in this paper, however, that going beyond 20% can be achieved on an

evolutionary path again. It is therefore the main purpose of this abstract to give quantitative foundations for choosing the new PERC production equipment so it stays useful in the near future for achieving 22% efficiency. For our predictions, we use state-of-the-art SENTAURUS [1] device modelling, combined with the EDNA and GRID calculators [2], and SPICE models.

## 2. Reaching 22% efficiency on a standard path

From the Shockley diode equation, it follows that to reach 22% efficiency, the total saturation current  $J_0$  must be no more than 200 fA/cm<sup>2</sup>. This conclusion arises by assuming  $J_{sc} = 40$  mA/cm<sup>2</sup>, an ideality factor  $m = 1$ , and a total  $R_s = 0.4 \Omega \cdot \text{cm}^2$ . (A lower  $J_0$  is required if  $m > 1$  or if  $R_s$  is larger.) Since the Shockley equation serves only as a rough guide, we do not discuss its assumptions.

Having set an upper limit to the  $J_0$  of a 22% solar cell, we next set a target  $J_0$  for the three major components of the solar cell: the emitter  $J_{0e}$ , the base  $J_{0,base}$ , and the rear  $J_{0,rear}$ . We can then examine how those targets might be met by today’s equipment—or perhaps tomorrow’s equipment.

In the following example, the target  $J_0$  of the three components is chosen to be  $J_{0e} \approx 80$ ,  $J_{0,base} \approx 50$ , and  $J_{0,rear} \approx 70$  fA/cm<sup>2</sup>, but there is freedom in dividing the components.

### 2.1. Constraints on the emitter

The  $J_{0e}$  of today’s emitters is about 150-200 fA/cm<sup>2</sup>. In our quest for  $J_{0e} = 80$  fA/cm<sup>2</sup> and a 22% solar cell, it must be substantially improved. The  $J_{0e}$  depends not only on the emitter’s dopant profile, but also on the amount of phosphorus precipitates [3] introduced during fabrication, and on the quality of the surface passivation [4].

Because it is difficult to reach 22% cell efficiency with a homogeneous emitter and conventional screen-printing, we choose a selective emitters.  $J_{0e}$  consists of three parts: the metal contacts  $J_{0,met}$ , the passivated n<sup>++</sup> part  $J_{0,n^{++}}$ , and the passivated n<sup>+</sup> part  $J_{0,n^+}$ , which sum to give  $J_{0e}$  respective to their area fraction:

$$J_{0e} = \frac{w_{met}}{p_f} J_{0,met} + \frac{w_{n^{++}}}{p_f} J_{0,n^{++}} + \frac{p_f - w_{met} - w_{n^{++}}}{p_f} J_{0,n^+} \tag{1}$$

where  $p_f$  is the front finger pitch,  $w_{met}$  and  $w_{n^{++}}$  are the width of the contact or n<sup>++</sup> region, respectively. In the following, we assume that the emitter is fabricated with a POCl<sub>3</sub> diffusion, and we use the experimental values from a recent study [5] shown in Fig. 1(a). Using these values, we optimise Eq. (1) and cross-check with SENTAURUS.

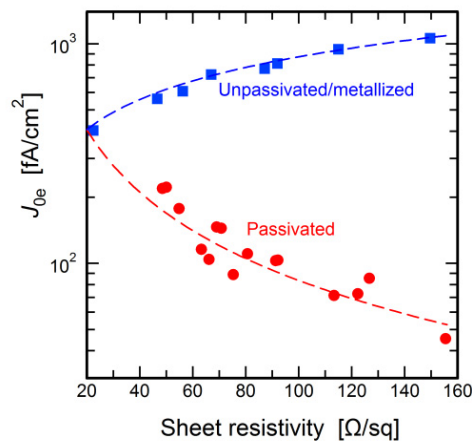


Fig.1. Experimentally achieved  $J_{0e}$  by POCl<sub>3</sub> diffusions [5] in dependence of  $\rho_{em}$ .

For the simulation of selective emitters, we examine how the  $J_{0e}$  depends on two technological constraints. Firstly, the alignment tolerance of the metal fingers  $w_{tol}$  (in units of  $\mu\text{m}$ ) is varied; this tolerance implies that the  $n^{++}$  region must be wider than the metal contact by  $w_{tol}$ . And secondly, the width of the metal contacts  $w_f$  is varied. Fig. 2 presents the results, giving a contour plot of  $J_{0e}$  and  $\rho_{n^{++}}$  as a function of  $w_{tol}$  (x-axis) and  $w_f$  (y-axis). It was simulated for  $p_f = 1.1 \text{ mm}$ ,  $J_{0,n^+} = 60 \text{ fA/cm}^2$  and  $\rho_{n^+} \approx 120 \text{ }\Omega/\text{sq}$ .

In Fig. 2, we see that as  $w_{tol}$  decreases, the optimum  $\rho_{n^{++}}$  decreases and a lower  $J_{0e}$  is attained. We find that, for example, the total  $J_{0e} = 80 \text{ fA/cm}^2$  (or  $90 \text{ fA/cm}^2$ ) can indeed be achieved with  $60 \mu\text{m}$  wide metal contacts, if the alignment tolerance is maximally  $w_{tol} \approx 50 \mu\text{m}$  (or  $90 \mu\text{m}$ ). In this case,  $\rho_{n^{++}} \approx 40 \text{ }\Omega/\text{sq}$  (or  $\approx 50 \text{ }\Omega/\text{sq}$ ) is optimum. Note, how sensitively the  $w_{tol}$  impacts on  $J_{0e}$ . However, an alignment tolerance down to  $30 \mu\text{m}$  seems to be feasible [6].

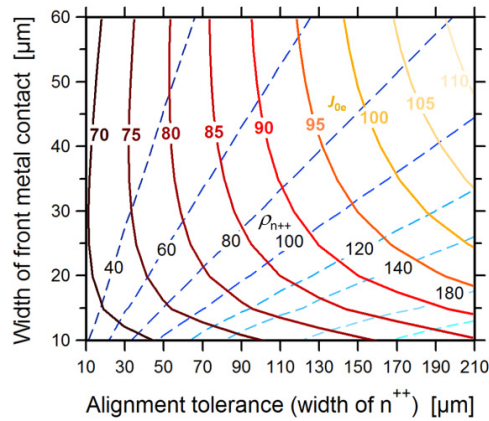


Fig. 2. Simulation of a selective emitter with  $J_{n^+} = 60 \text{ fA/cm}^2$ . The minimally achievable total  $J_{0e}$  (solid lines) is plotted with its corresponding optimum  $\rho_{n^{++}}$  (dashed lines), in dependence of the alignment tolerance of the front metal finger, and the width of the front contact (the technological restrictions). A front finger distance of  $p_f = 1.1 \text{ mm}$  is assumed (from Fig. 3).

## 2.2. Optimization of the metal grid

Optimizing the finger pitch is the next task. It affects the resistive losses in the emitter and in the front metallization, as well as  $J_{sc}$ , and is therefore a highly non-linear optimization task. The series resistance contribution (in units of  $\Omega\text{cm}^2$ ) of the selective emitter can be calculated as

$$R_{s.em} = \frac{1}{3l_f(2n_f 2n_{bb})L^2} \left[ \rho_{n^{++}} L_{n^{++}} L^2 \left( 1 + \frac{L_{n^+}}{L} + \frac{L_{n^+}^2}{L^2} \right) + \rho_{n^+} L_{n^+} L_{n^+}^2 \right] A_{cell} \quad (2)$$

where  $l_f$  is the finger length,  $n_f$  ( $n_{bb}$ ) is the number of fingers (busbars) in the cell,  $L$  is half of the finger separation (which is the longest way electrons travel laterally in the emitter),  $A_{cell}$  the cell area, and there is  $L_{n^+} = w_{n^+}/2$ ,  $L_{n^{++}} = w_{n^{++}}/2$ , and  $L = p_f - w_{met}$ .

We now determine how the efficiency of the solar cell depends on technological constraints placed by the screen-printing technology. The results are plotted in Fig. 3(a), which plots efficiency contours against the finger width  $w_f$  (x-axis) and the finger height (y-axis). In these simulations, series resistance contribution of the metal grid is calculated with the freeware GRID [7] for a standard resistivity of screen-printed Ag fingers of  $4.5 \times 10^{-6} \text{ }\Omega\text{cm}$ ; the shading is assumed to be 50% of the finger coverage and 90% of the busbar coverage, as was measured in a module [8]. For each simulation, the optimal finger pitch is selected, as plotted by dashed lines.

Fig. 3(a) shows that with  $60 \mu\text{m}$  wide and about  $25 \mu\text{m}$  high fingers, 22% is possible if the front finger pitch  $p_f$

is about 1.1 mm. Narrower fingers (and accordingly smaller  $p_f$ ) are only necessary if going above 22% cell efficiency, and instead, multi-wire busbars would be similarly effective.

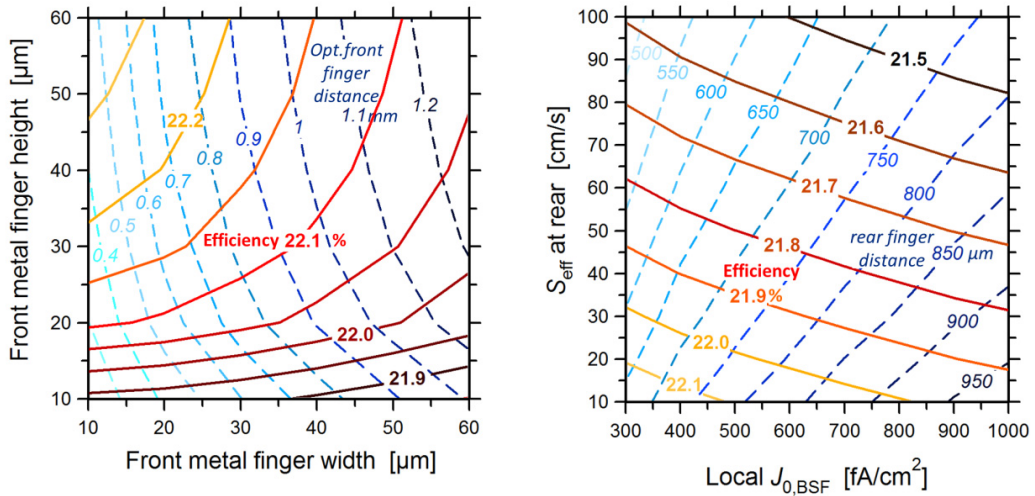


Fig. 3. (a) Predicted optimum front finger pitch  $p_f$  (blue dashed lines) with the resulting maximally achievable cell efficiency (red solid lines) in dependence of the front finger width and front finger height (the technological restrictions). (b) Simulated demands of the rear metallisation, BSF and passivation: the optimum rear finger pitch (blue dashed lines) with the resulting maximally achievable cell efficiency (red lines). Note that these predictions depend on the emitter quality.

### 2.3. Optimization of the rear

To achieve 22% cell efficiency, the losses in the local BSFs and at the rear surface should combine to give a  $J_{0,\text{rear}}$  of no more than 70 fA/cm<sup>2</sup> (as stated in the beginning). Fig. 3(b) shows how this may be achieved assuming 30 μm wide rear contact openings. For example, a  $J_{0,\text{rear}}$  of 70 fA/cm<sup>2</sup> and therefore an efficiency of 22.0% arises when  $J_{0,\text{BSF}} \approx 800$  fA/cm<sup>2</sup> and  $S_{\text{eff}} \approx 10$  cm/s, where the latter has been experimentally demonstrated for Al<sub>2</sub>O<sub>3</sub>/SiN<sub>x</sub> passivation. In these simulations, the rear finger pitch that yields the maximised efficiency is selected—this is plotted as the dashed lines in Fig.3(b). In the example case, the optimum rear finger distance then is 850 μm, but it may be chosen as wide as 1.2 mm without compromising on cell efficiency (not shown here).

We note that with  $S_{\text{eff}} = 100$  cm/s, only 21.5% efficiency is achievable, unless the emitter or the front metallization are made better than in the example of Fig. 2.

### 2.4. Wafer quality requirements

In all of our simulations, we assume a SRH lifetime  $\tau$  in the wafer of 1 – 2 ms. With lower  $\tau$ , the equivalent  $J_{0,\text{base}}$  exceeds 40 fA/cm<sup>2</sup>. This lifetime is presently achievable in boron-doped Cz materials by applying deactivation procedures [9]. It has been also achieved in Ga-doped or magnetic Cz materials.

## 3. Conclusions

To reach 22% cell efficiency, 60 μm wide and 25 μm high front metal fingers with a pitch of about 1.1 mm are sufficient, if an emitter saturation current density  $J_{0e} = 80$  fA/cm<sup>2</sup> (including contacts) is realized, e.g. by a selective emitter with 60 μm wide n<sup>++</sup> regions (with  $\rho_{n^{++}} \approx 40$  Ω/sq), and with an n<sup>+</sup> region that has  $J_{0,n^+} = 60$  fA/cm<sup>2</sup>, and  $\rho_{n^+} \approx 120$  Ω/sq. At the rear,  $S_{\text{eff}} < 30$  cm/s is favourable, as otherwise the front must be improved to compensate. Such a rear structure may be realised by a passivation with  $S = 10$  cm/s, about 30 μm wide openings with a pitch near 1 mm, and local Al-BSFs with  $J_{0,\text{BSF}} < 700$  fA/cm<sup>2</sup>. The main issue is the bulk lifetime  $\tau$ : it must reach about 2 ms at the

prevailing excess carrier densities at MPP, which are near  $1 \times 10^{13} \text{ cm}^{-3}$  (and at open-circuit conditions about  $2 \times 10^{15} \text{ cm}^{-3}$ ) in  $1 \Omega \text{ cm}$  material.

## References

- [1] Sentaurus User Manual, Synopsys Inc., Mountain View, CA, 2013.
- [2] McIntosh KR, Altermatt PP. A freeware 1D emitter model for silicon solar cells. 35th IEEE PVSC, Honolulu, 2010, pp. 2188–2193. Freely available online: [www.pvlighthouse.com.au](http://www.pvlighthouse.com.au)
- [3] Min B, Wagner W, Dastgheib-Shirazi A, Altermatt PP. Limitation of industrial phosphorus-diffused emitters by SRH recombination. This conference.
- [4] Altermatt PP, Schumacher JO, Cuevas A, Kerr MJ, Glunz SW, King RR, Heiser G, Schenk A. Numerical modelling of highly doped Si:P emitters based of Fermi-Dirac statistics and self-consistent material parameters. *J Appl Phys* 2002;92:3187–97.
- [5] Fischer B, Müller J, Altermatt PP. A simple emitter model for quantum efficiency curves and extracting the emitter saturation current. 28th EU Photovoltaic Solar Energy Conference, Paris, France; 2013. p. 840–45.
- [6] Voltan A, Galiazzo M, Tonini D, Casarin A, Cellere G and Baccini A. Advanced alignment technique for precise printing over selective emitter in c-Si solar cells. *Prog PV* 2012;20:670–80.
- [7] Grid calculator, freely available online: [www.pvlighthouse.com.au](http://www.pvlighthouse.com.au)
- [8] Woehl R, Hörteis M, Glunz SW. Determination of the effective optical width of screen-printed and aerosol-printed and plated fingers. 23rd EU Photovoltaic Solar Energy Conference, Valencia, Spain; 2008. p. 1377–80.
- [9] Walter DC, Lim B, Bothe K, Voronkov VV, Falster R, Schmidt J. Effect of rapid thermal annealing on recombination centres in boron-doped Czochralski-grown silicon. *Appl Phys Lett* 2014;104:042111.